

Application of a novel redox-active electrolyte in MnO₂-based supercapacitors

YU HaiJun, WU JiHuai*, FAN LeQing, LIN YouZhen, CHEN ShuHong, CHEN Yuan, WANG JiangLi, HUANG MiaoLiang, LIN JianMing, LAN Zhang & HUANG YunFang

Engineering Research Center of Environment-Friendly Functional Materials, Ministry of Education; Institute of Materials Physical Chemistry, Huaqiao University, Quanzhou 362021, China

Received July 14, 2011; accepted November 21, 2011; published online June 20, 2012

This paper reports a novel strategy for preparing redox-active electrolyte through introducing a redox-mediator (*p*-phenylenediamine, PPD) into KOH electrolyte for the application of ball-milled MnO₂-based supercapacitors. The morphology and compositions of ball-milled MnO₂ were characterized using scanning electron microscopy (SEM) and X-ray diffraction (XRD). The electrochemical properties of the supercapacitor were evaluated by cyclic voltammetry (CV), galvanostatic charge-discharge (GCD), and electrochemical impedance spectroscopy (EIS) techniques. The introduction of *p*-phenylenediamine significantly improves the performance of the supercapacitor. The electrode specific capacitance of the supercapacitor is 325.24 F g⁻¹, increased by 6.25 folds compared with that of the unmodified system (44.87 F g⁻¹) at the same current density, and the energy density has nearly a 10-fold increase, reaching 10.12 Wh Kg⁻¹. In addition, the supercapacitor exhibits good cycle-life stability.

supercapacitor, redox-active electrolyte, manganese dioxide, *p*-phenylenediamine, pseudocapacitance

1 Introduction

The development of high-performance energy storage devices is an effective measure to face the increasing requirements of modern electronic products. Supercapacitors [1], also called electrochemical capacitors, double electric layer capacitors or ultracapacitors, have aroused wide research interest due to their high power capability and long durability (>10⁵ cycles). However, the low energy density limits their application in many important fields [2]. Recently, the researches for improving the performances of supercapacitors mainly focus on the electrode materials and electrolytes.

Much work has been done to fabricate high-performance supercapacitors based on Faradic pseudocapacitive mecha-

nism, such as RuO₂ [3], MnO₂ [4–6], Fe₃O₄ [7] and NiO_x [8]. MnO₂ was regarded as the most potential pseudocapacitive electrode material, due to its low price, stable and environment-friendly features. There are some methods for preparing MnO₂ electrode materials [9, 10], however the current methods are complicated and rigorous conditions [5, 6]. Therefore, it is significant to explore a simple and facile route for preparing a high-efficiency and stable MnO₂-based supercapacitor.

Recently, an innovative redox-active electrolyte has been reported, which efficiently enhances the capacitive performance of supercapacitors. Zhang *et al.* [11] added hexacyanoferrate (II) and (III) jointly into KOH aqueous solution as electrolyte for the supercapacitor. Because the Fe(CN)₆^{3-/4-} ion pair acts as an electron relay in the system, the capacitive property of the supercapacitor was improved, but the supercapacitor showed a poor cyclic stability. Li *et al.* [12] reported a Cu(II)-ionic liquid electrolyte for car-

*Corresponding author (email: jhwu@hqu.edu.cn)

bon-based supercapacitor. The redox process of $\text{Cu}^{2+}/\text{Cu}^0$ in an electrolyte obviously improved the properties of ionic liquid electrolyte and the corresponding carbon-based supercapacitor. Besides, Santamair *et al.* [13] reported an acidic redox-active electrolyte. The reversible redox reaction of hydroquinone in the acid system apparently increases the specific capacitances of all carbon-based supercapacitors. Moreover, Zhou *et al.* [14,15] added NaI/I_2 into polymer gel electrolyte and activated carbon composite, the performances of the supercapacitor increased. Nevertheless, the comprehensive performances of supercapacitors still need to be improved.

In this study, *p*-phenylenediamine (PPD), a redox mediator which is extensively researched in the field of biomedicine and electroanalysis, was directly introduced into conventional KOH aqueous solution to form a redox-active electrolyte for MnO_2 -based supercapacitors. Due to the introduction of PPD, the electrochemical properties of the MnO_2 -based supercapacitor were improved efficiently.

2 Experimental

2.1 Reagents and instruments

Manganese dioxide (MnO_2), potassium hydroxide (KOH), graphite, *p*-phenylenediamine (PPD) and *N*-methyl-2-pyrrolidone (NMP) were purchased from Sinopharm Chemical Reagent Co., Ltd. Polytetrafluoroethylene (PTFE) and nickel foam were purchased commercially from Guangzhou Xingshengjie Science Technology Co., Ltd. and Changsha Lyrun New Material Co., Ltd., respectively. All materials were analytical reagents and used without further treatments.

The instruments included a planet balling mill (ND6-2L, Nanjing Nanda Tianzun electronic Co., Ltd.), scanning electron microscopy (SEM, Hitachi S-4800, Hitachi Science System Ltd., Japan), X-ray diffraction spectro-meter (XRD, D8 Advance, Bruke Inc., Germany), and an electrochemical workstation system (CHI660C, Shanghai Chen Hua Co., Ltd.).

2.2 The preparation of redox-active electrolytes

PPD with different mass (0.010, 0.025, 0.050, 0.075, 0.100 g) was added into 10 ml KOH electrolyte (1.78 mol L^{-1}) with agitation. After complete dissolution, the redox-active electrolytes (E1, E2, E3, E4, and E5) were obtained. For comparison, the KOH electrolyte (E0) with the same molar concentration was also adopted.

2.3 The preparation of MnO_2 electrode

7 g of MnO_2 , 3 g of graphite and 100 g of stainless steel balls were put into the planet balling mill. After ball milling for 10 h, a nanoscale mixture of MnO_2 /graphite was ob-

tained.

The MnO_2 /graphite mixture and PTFE were mixed with a mass ratio of 95: 5 and dispersed in NMP. The resultant mixture was ground and the NMP was removed by ultrasonic vibrating and heating to get uniform slurry. The slurry was pressed by Decal method to form a thin sheet. Under pressure of 10 MPa, the thin sheet was painted on nickel foil. After drying at 100°C for 24 h in a vacuum oven, a MnO_2 electrode was thus obtained.

2.4 Fabrication of supercapacitor

The supercapacitors (S1, S2, S3, S4, and S5) were fabricated by using two same MnO_2 electrodes and different redox-active electrolytes. At the same time, the same MnO_2 -based supercapacitor with E0 electrolyte was also assembled.

2.5 Measurements and characterizations

The morphology and structure of MnO_2 were observed and photographed by SEM and XRD, respectively. The electrochemical performances of supercapacitors were characterized by cyclic voltammetry (CV), electrochemical impedance spectroscopy (EIS), and galvanostatic charge-discharge (GCD) measurements. All tests were performed on CHI 660C at room temperature.

The specific capacitance of the supercapacitor (C , F g^{-1}), power density (P , W kg^{-1}), and energy density (E , Wh kg^{-1}) were calculated according to the following equations:

$$C = \frac{I \times \Delta t}{\Delta V \times m_{\text{ac}}} \quad (1)$$

$$E = \frac{C \times \Delta V^2}{2} \times \frac{1000}{3600} \quad (2)$$

$$P = 1000 \times \frac{E}{\Delta t} \quad (3)$$

$$C = 1000 \times \frac{i}{m_{\text{ac}} \times v} \quad (4)$$

where I (ampere) is the working current, m_{ac} (grams) is the weight of the active material (including the binder and the graphite), Δt (seconds) is the charge-discharge time, i (A) is peak current, and v (mV/s) is the sweep rate of CV test. ΔV (volts) is the actual voltage after eliminating the iR_{drop} (volts), which is defined as the electrical potential difference between the two ends of a conducting phase during charging-discharging. The specific capacitances of the electrode (C_s) were obtained by multiplying C by four.

3 Results and discussion

3.1 The structural analysis of MnO_2

The XRD patterns of graphite and raw MnO_2 before ball

milling, and MnO₂/graphite composite after ball milling are shown in Figure 1, the close-up view of the left part in the low degree. It is shown that the maximal diffraction peak of graphite decreases after ball milling, which may be ascribed to the destruction of the crystal structure. Due to the reduction of thickness and dimension of graphite, the composite has a better conductivity [19]. The XRD patterns of MnO₂/graphite and MnO₂ (β -MnO₂) indicate that all the positions of maximal diffraction peaks for MnO₂ are not changed except apparent strengthening at 37.33°, which indicates that the crystalline structure of MnO₂ is not destroyed after ball milling [20].

3.2 Morphology observation of MnO₂

Figure 2 shows the typical SEM images of MnO₂ in different magnification before and after ball milling treatment. It is shown that the MnO₂ particle size are between 30 and 40 μm before ball milling (a). After ball milling, the size of MnO₂ particles has apparently decreased, and reaching nanoscale (50–200 nm), as shown in Figure 2(b).

3.3 GCD measurements

In order to get the optimum redox-active electrolyte, C_s of supercapacitors based on various electrolytes (E1, E2, E3, E4, and E5) is counted by GCD test and the results are shown in Table 1. It is observed that C_s of supercapacitors increases with the increases of PPD amount; when PPD amount is 0.050 g, C_s reaches the largest value (325.24 F g⁻¹). Beyond 0.050 g, C_s decreases with the increases of PPD concentration. The concentration of PPD is not high enough to improve the capacitive performance, but higher concentration of PPD will lead to the aggregation of free ions and charges in the system, which decreases the performances of supercapacitors. Therefore, the 0.050 g (E3) PPD is suitable.

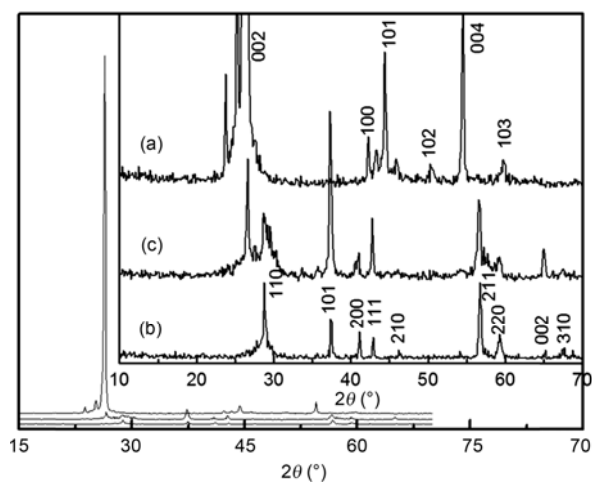


Figure 1 XRD patterns of materials. (a) Graphite; (b) MnO₂ before ball milling; (c) MnO₂/graphite mixture after ball milling.

Table 1 The influence of PPD on C_s of supercapacitors

PPD (g)	C_s of supercapacitors (F g ⁻¹)
0.010	260
0.025	290.56
0.050	325.24
0.075	310.01
0.100	300.35

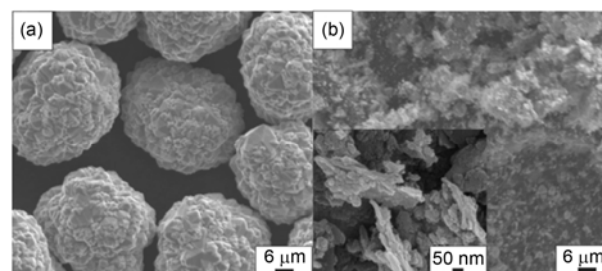


Figure 2 SEM photographs of materials. (a) The MnO₂ before ball milling; (b) the MnO₂/graphite mixture after ball milling.

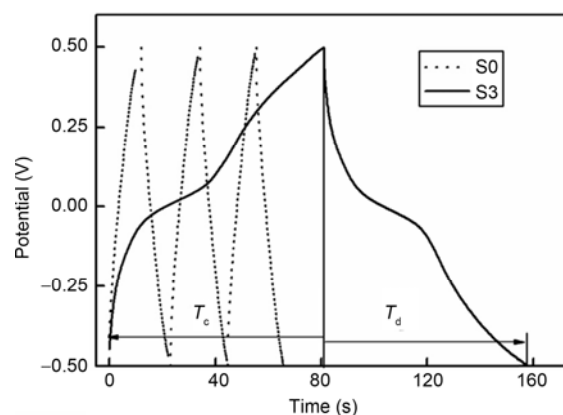


Figure 3 GCD curves of S0 and S3. Current density: 1 A g⁻¹.

The GCD curves for S0 and S3 are compared in Figure 3. It is shown that the charge time (T_c) and discharge time (T_d) of the supercapacitors are almost equal, implying both of them have good columbic efficiency (Figure 3) [21]. Moreover, it is interesting that the charge-discharge time of S3 is much longer than that of S0, revealing a great improvement of the performances of the supercapacitor. According to eq. (1), under a charging-discharging current density of 1 A g⁻¹, C_s of S0 and S3 is determined to be 44.87 and 325.24 F g⁻¹, respectively. C_s for the redox-active electrolyte is increased by 6.25 folds compared with that of the current KOH system. The quick and reversible redox reactions of PPD in the electrolyte system may be the main reason for the long discharge time for the S3.

In Figure 4, the C_s for S0 and S3 at different current densities and scan rates are presented. For the GCD test, the C_s of the two supercapacitors increase with the increasing of current density, when the current density is 5 A g⁻¹, C_s of

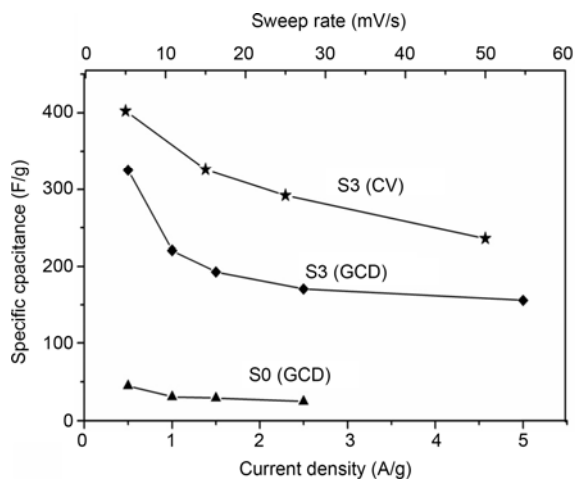


Figure 4 The specific capacitance of S0 and S3 at different current densities and scan rates.

S3 reaches 175.81 F g^{-1} with a capacitive retention of 54.05%. Similarly, with the increasing of scan rate of $C-V$ test, C_s of two supercapacitors also decline smoothly. From these results, we conclude that S3 not only shows better electrochemical properties, but also still keeps a relatively high capacitive retention. Ragone of energy density and power density of supercapacitors are shown in Figure 5. According to eqs. (2) and (3), the energy density of S0 (E_{S0}) and S3 (E_{S3}) were counted to be 10.12 and 1.29 Wh Kg^{-1} at 1 A g^{-1} , respectively, which increases by nearly 10 folds. The power density of S0 (P_{S0}) and S3 (P_{S3}) were 474 W kg^{-1} and 455 W kg^{-1} , respectively. It can be inferred that redox-active mediator is an efficient method for improving the performances of supercapacitors.

3.4 $C-V$ tests

$C-V$ tests for the S0 and S3 at a scan rate of 5 mV s^{-1} are shown in Figure 6. The $C-V$ curves of S3 display shapes with one pair of well-defined redox peak (P/P') centered at 0 V and nearly same peak currents (5.11 and 5.03 mA), which indicates the good reversibility of the redox mediator

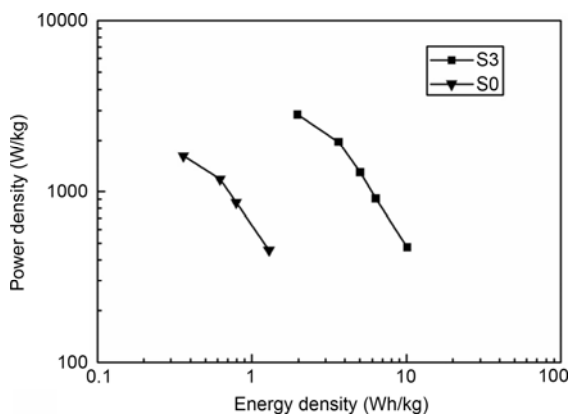


Figure 5 Ragone of energy density and power density.

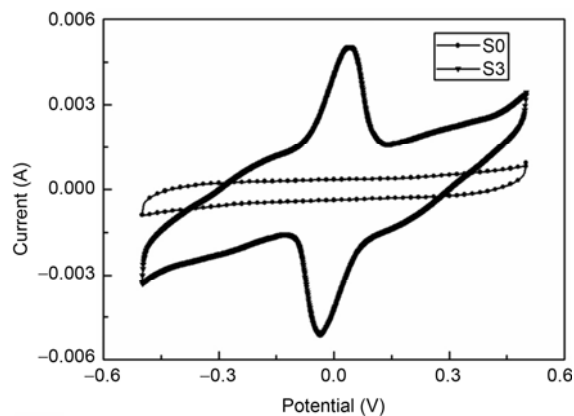


Figure 6 $C-V$ curves for S0 and S3 at a scan rate of 5 mV s^{-1}

in the electrolyte. The redox peak (P/P') of S3 corresponds to the redox transformation of p -phenylenediamine and p -phenylenediimine on the MnO_2 electrode|electrolyte interface [13]. However, the $C-V$ curves of S0 display a quasi-rectangle shape without apparent redox peak, implying an ideal electric double layer capacitor [22]. Besides, the capacitances are proportional to the areas of $C-V$ shapes [23], and the appearance of bumps means that the capacitances of S3 have been improved about 6 folds, which is attributed to the pseudocapacitances produced by redox reactions of PPD. On the basis of $C-V$ tests, the good performance of S3 is due to the capacity-storage mechanism of the electrical double layer capacitance and Faradic pseudocapacitance produced by the redox reaction of p -phenylenediamine/ p -phenylenediimine on the MnO_2 electrode|electrolyte interface.

3.5 EIS technique

Figure 7 shows the Nyquist plots of S0 and S3. Both supercapacitors exhibit ideal electrochemical capacitance behaviors. In the high frequency region, S3 not only has lower inner resistance (1.87Ω for S3 and 4.32Ω for S0, respectively) calculated from the point of intersecting with the x -axis, but also has smaller charge transfer resistance (2.87Ω for S3 and 4.68Ω for S0, respectively), which was counted from the span of the single semi-circle along the x -axis. It can be inferred that the introduction of PPD decreases the inner resistance and accelerates the transfer of ions. Subsequently, the quick charge discharge ability of the supercapacitor was improved. Furthermore, in the low frequency region, the imaginary part of S3 is more perpendicular to the real part. In brief, the introduction of PPD improves the impedance performance of the supercapacitor.

3.6 Cycle-life testing

The long cyclic durability is a crucial problem for supercapacitors. The cycle stability of S0 and S3 was also evaluated

at a current density of 1 A g^{-1} for 5000 cycles, as shown in Figure 8. The C_s of S0 displays good cyclic ability with a slight decrease after 5000 cycles, which implies the MnO_2 electrode exhibits good electrochemical stability. The C_s of S3 declines quickly at the beginning of the 2000th cycle, and then keeps a stable value about 75% of the initial value. The decrease of capacitance in the long-term cycling may be due to the incomplete redox reactions of PPD in the electrolytic system.

4 Conclusion

We reported a novel strategy for preparing redox-active electrolyte through introducing a redox mediator (PPD) into KOH electrolyte for the application of nano- MnO_2 -based supercapacitors. The supercapacitor exhibits excellent electrochemical performances with a high electrode specific capacitance of 325.24 F g^{-1} and energy density of 10.12 Wh Kg^{-1} . In addition, the supercapacitor shows good cycle-life stability. It is believed that the simple and high-efficient

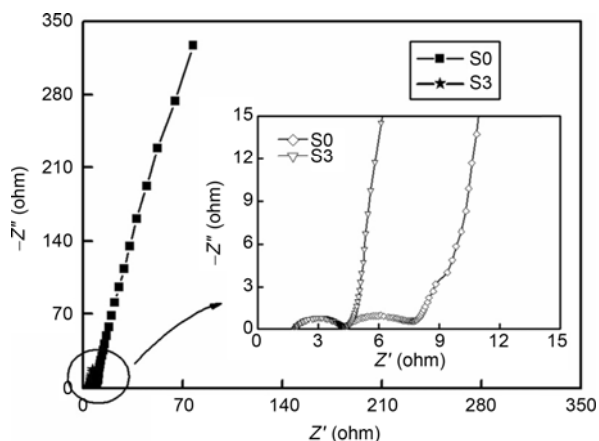


Figure 7 Nyquist plots of S0 and S3, the close-up view of the left plot in the high frequency region.

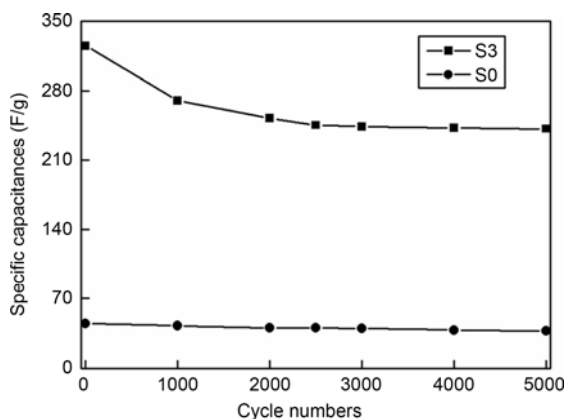


Figure 8 Variation of the C_s of S0 and S3 during the long-term cycle.

redox-mediated dope provides a potential measure for the realization of high-energy-storage devices.

This work was supported by the National High Technology Research and Development Program of China (2009AA03Z217), the National Natural Science Foundation of China (90922028, 50842027) and the Key Project of Ministry of Education of China (211204).

- Conway BE. *Electrochemical Supercapacitors: Scientific Fundamentals and Technological Applications*, 2nd. New York: Kluwer Academic/ Plenum Publishers, 1999
- Lang XY, Hirata A, Fujita T, Chen MW. Nanoporous metal/oxide hybrid electrodes for electrochemical supercapacitors. *Nat Nano*, 2011, 6: 232–236
- Hu CC, Chang KH, Lin MC, Wu YT. Design and tailoring of the nanotubular arrayed architecture of hydrous RuO_2 for next generation supercapacitors. *Nano Lett*, 2006, 6: 2690–2695
- Hu CC, Hung CY, Chang KH, Yang YL. A hierarchical nanostructure consisting of amorphous MnO_2 , Mn_3O_4 nanocrystallites, and single-crystalline MnOOH nanowires for supercapacitors. *J Power Sources*, 2011, 196: 847–850
- Wei WF, Cui XW, Chen WX, Ivey DG. Manganese oxide-based materials as electrochemical supercapacitor electrodes. *Chem Soc Rev*, 2011, 40: 1697–1721
- Ni JP, Lu WC, Zhang LM, Yue BH, Shang XF, Lv Y. Low-temperature synthesis of monodisperse 3D manganese oxide nanoflowers and their pseudocapacitance properties. *J Phys Chem C*, 2008, 113: 54–60
- Zhao X, Johnston C, Crossley A, Grant PS. Printable magnetite and pyrrole treated magnetite based electrodes for supercapacitors. *J Mater Chem*, 2010, 20: 7637–7644
- Meher SK, Justin P, Ranga RG. Microwave-mediated synthesis for improved morphology and pseudocapacitance performance of nickel oxide. *ACS Appl Mater Inter*, 2011, 3: 2063–2073
- Feng Y, Zhang ML, Chen Y, Han Y, Shi ZH. Inorganic salt water solution reaction synthesis and capacitor characteristics of nano- MnO_2 powder. *J Chin Cera Soc*, 2005, 33: 318–322 (in chinese)
- Wang HQ, Yang GF, Li QY, Zhong XX, Wang FP, Li ZS, Li YH. Porous nano- MnO_2 : Large scale synthesis via a facile quick-redox procedure and application in a supercapacitor. *New J Chem*, 2011, 35: 469–475
- Su LH, Zhang XG, Mi CH, Gao B, Liu Y. Improvement of the capacitive performances for Co-Al layered double hydroxide by adding hexacyanoferrate into the electrolyte. *Phys Chem Chem Phys*, 2009, 11: 2195–2202
- Sun GH, Li KX, Sun CG. Electrochemical performance of electrochemical capacitors using Cu(II)-containing ionic liquid as the electrolyte. *Micropor Mesopor Mat*, 2010, 128: 56–61
- Roldán S, Blanco C, Granda M, Menéndez R, Santamaría R. Towards a further generation of high-energy carbon-based capacitors by using redox-active electrolytes. *Angew Chemie Int Ed*, 2011, 50: 1699–1701
- Yin YJ, Zhou JJ, Mansour AN, Zhou XY. Effect of NaI/I_2 mediators on properties of PEO/ LiAlO_2 based all-solid-state supercapacitors. *J Power Sources*, 2011, 196: 5997–6002
- Wu JH, Lan Z, Lin J, Huang ML, Hao SC, Sato T, Yin S. A novel thermosetting gel electrolyte for stable quasi-solid-state dye-sensitized solar cells. *Adv Mater*, 2007, 19: 4006–4011
- Ke NJ, Lu SS, Cheng SH. A strategy for the determination of dopamine at a bare glassy carbon electrode: *p*-phenylenediamine as a nucleophile. *Electrochem Commun*, 2006, 8: 1514–1520
- Li M, Yang CY, Zhou WK, Zhu M. Reversible oxidation of *p*-phenylenediamine on hemoglobin /poly(L-glutamic acid) /glassy carbon modified electrode. *Chinese J App Chem*, 2010, 9: 1093–1098 (in chinese)

- 18 Jiao K, Sun W, Zhang SS, Sun G. Application of p-phenylenediamine as an electrochemical substrate in peroxidase-mediated voltammetric enzyme immunoassay. *Anal Chim Acta*, 2000, 413: 71–78
- 19 Zhao WF, Fang M, Wu FR, Wu H, Wang LW, Chen GH. Preparation of graphene by exfoliation of graphite using wet ball milling. *J Mater Chem*, 2010, 20: 5817–5819
- 20 Zhang WX, Yang ZH, Wang X, Zhang YC, Wen XG, Yang SH. Large-scale synthesis of β -MnO₂ nanorods and their rapid and efficient catalytic oxidation of methylene blue dye. *Catal Commun*, 2006, 7: 408–412
- 21 Hashmi SA, Kumar A, Tripathi SK. Investigations on electrochemical supercapacitors using polypyrrole redox electrodes and PMMA based gel electrolytes. *Eur Polym J*, 2005, 41: 1373–1379
- 22 Toupin M, Brousse T, Bélanger D. Charge storage mechanism of MnO₂ electrode used in aqueous electrochemical capacitor. *Chem Mater*, 2004, 16: 3184–3190
- 23 Li F, Shi JJ, Qin X. Synthesis and supercapacitor characteristics of PANI/CNTs composites. *Chinese Sci Bull*, 2009, 54: 3900–3905 (in chinese)